


Remote Sensing of Soil-Plant-Atmosphere Processes

By:
Yonatan Schwartz

Code link:

 SPAP_Final_Project.ipynb

1. Introduction

Remote sensing provides a profound understanding of ecological processes and energy dynamics within the complex soil-plant-atmosphere continuum.

Within this framework, the calculation of **net radiation (R_n)** and the components of the energy balance, such as **ground heat flux (G)**, **sensible heat flux (H)**, and **latent heat flux (LE)**, are central tools for assessing key physical processes, including evapotranspiration (ET).

The energy balance equation, $R_n = G + H + \lambda E$, describes the balance between incoming and outgoing radiation and the energy fluxes absorbed and emitted by the soil and vegetation. Agricultural systems use this information to assess water requirements, determine optimal irrigation levels, and improve resource management based on changing field and climatic conditions. Satellites such as MODIS, COPENICUS, and MSG provide critical data for calculating these parameters.

R_n - measured by satellite sensors, which enables the estimation of the energy entering and leaving the system

G - describes the energy absorbed or emitted by the soil, related to soil temperature changes.

H -represents heat exchange between the soil and atmosphere, primarily through air movement.

LE -is directly linked to the processes of evaporation and transpiration, allowing the assessment of water evaporating from plants and soil.

This project examined various methods for calculating radiation and energy fluxes, utilizing remote sensing data from satellites such as MODIS and MSG, and physical models like the Weather Research and Forecast Model (WRF). This analysis provides insights into the energy and water dynamics across large geographic areas, focusing on two specific dates in **2018 (March 22 and August 24)**. The project compares the results between the two dates and discusses the implications for climate and agricultural management.

2. Methods

In this part, I will present the calculations of the energy balance equation's components:

R_n - Net radiation

$$R_n = G + H + \lambda E$$

The above equation is possible to represent in a better way which shows the wider components:

$$R_n = (1 - r_0) \cdot S \downarrow + L \downarrow - (1 - \epsilon_0) \cdot L \downarrow - \epsilon_0 \cdot \sigma \cdot T_0^4$$

r_0 = albedo

S = shortwave downwards

L = longwave downwards

ϵ_0 = emissivity

σ = Stefan-Boltzmann constant

T_0 = soil temp

Net radiation is the difference between the energy entering the system (from the sun) and the energy leaving it (primarily as heat radiated from the soil and vegetation).

R_n determines the total energy available for physical processes like evaporation, soil heating, and heat exchange with the atmosphere. Influenced by several factors, including solar angle, daylight hours, cloud cover, surface albedo (reflectivity), and thermal emissions. Positive net radiation means more energy is entering than leaving the system, contributing to soil heating or evaporation.

G- ground heat flux

$$G = 0.35 \left(e^{-\frac{0.5 LAI}{\sin \beta}} \cdot R_n \right) \cdot \cos(90 - \beta)$$

β = solar elevation angle

LAI = leaf area index

Ground heat flux represents the exchange of heat between the soil surface and the underlying layers. It describes the energy absorbed by or released from the soil, depending on its temperature and moisture content. This flux is closely related to the thermal properties of the soil and its ability to store or release energy.

H- sensible heat flux

$$H = \rho_a \cdot C_p \cdot \frac{T_0 - T_a}{r_{ah}}$$

ρ_a = moist air density

C_p = air specific heat at constant pressure [$J kg^{-1} K^{-1}$]

$T_0 - T_a$ = is the driving temperature gradient between the surface and reference height.

r_{ah} = aerodynamic resistance to heat transport between surface and reference level.

$$r_{ah} = \frac{1}{ku^*} \cdot \ln\left(\frac{Z_r - d}{h - d}\right) + \frac{h}{nk(h)} \cdot e^{[n(1 - \frac{z_0 + d}{n}) - 1]}$$

$$* u = \frac{k \cdot u(Z_r)}{\ln\left(\frac{Z_r - d}{z_0}\right)}$$

Sensible heat flux (H) refers to the transfer of heat between the soil surface and the atmosphere through conduction, driven by temperature differences. This flux is governed by factors such as soil and air temperatures, wind speed, and humidity. Sensible heat flux plays a significant role in influencing local air temperature and thermal comfort in different regions.

LE- latent heat flux

$$\lambda E = G + H + R_n$$

Due to the above calculations, the LE is easy to calculate.

Latent heat flux (LE) is the energy required for the evaporation of water from the soil and vegetation and for transpiration from plant leaves. This flux is critical in the water cycle and reflects the rate of evapotranspiration in agricultural areas. LE is directly influenced by soil moisture, air humidity, wind speed, and relative humidity.

ET- evapotranspiration

$$LE \left[\frac{W}{m^2} \right] = \rho_w \cdot I_v \cdot ET$$

$$\rho_w = 1000 \left[\frac{kg}{m^3} \right]$$

$$I_v = 2.5 \frac{MJ}{kg}$$

$$\left[\frac{W}{m^2} \right] = \frac{J}{s \cdot m^2} = 1000 \frac{kg}{m^3} \cdot 2.5 \cdot 10^6 \frac{J}{kg} \cdot \frac{1 \text{ day}}{86400 \text{ s}} \cdot 1 \frac{mm}{day} \cdot \frac{1m}{1000mm}$$

AOI- area of interest

The AOI I choose is the galilee due to its variety of landscape and land cover usage. The AOI is roughly 50 square km. The shapefile was created with QGIS and uploaded as an asset to GEE (Google Earth engine).

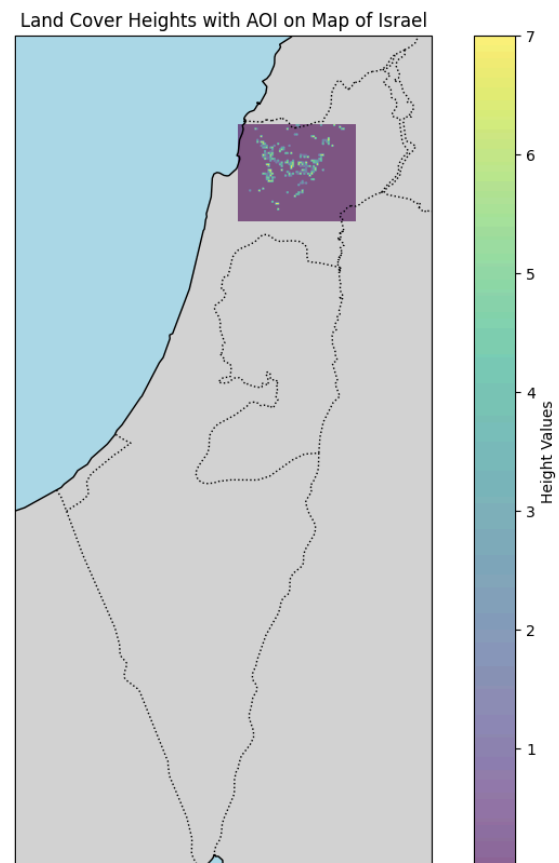


figure 1 - AOI - area of interest.

Data

Sensor/satellite	model dataset	variable	band
MODIS	MOD11A1	Surface temp	LST_Day_1km
		Emissivity	Emis_31
	MCD43A3	albedo	Albedo_WSA_vis
	MCD15A3H	Leaf Area Index	Lai
SEVIRI/MSG	MSG total and diffuse DSSF	downward surface shortwave flux	MDSSFTD
	MSG DSFL	downward surface longwave flux	MDSLFL
Copernicus	CGLS-LC100	Land cover	discrete_classification

Workflow and process

- Creation of AOI.
- Download MODIS, MSG, and Copernicus data to the +relevant AOI
- Download LSASAF files.
- Clip all files to the same reference file.
- Resample all files to the same reference file.
- All files are with the same dimensions - 53 x 62
- Applying scale factor and convert units.
- Apply mathematics as the above equations.
- Save and display.
- Flux results.

3. Results

Comparison of Rn, G, H, LE, and ET between the two dates:

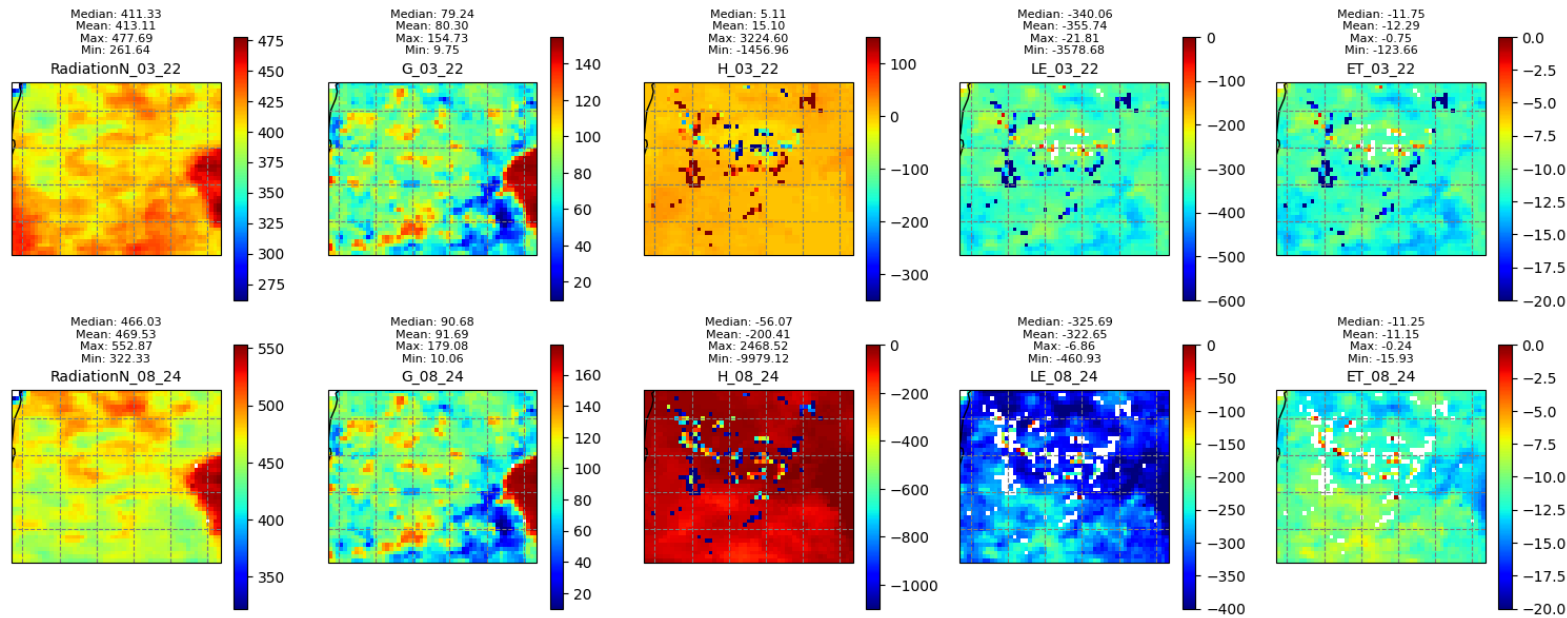


figure 2- calculated flux maps for Rn, G, H, LE, ET

The maps display the spatial distribution of five energy variables across two different dates: 03/22 and 08/24 2018. Each row in the image represents a different date, with **the top row depicting March and the bottom row depicting August**. Each column presents a different variable: net radiation (RadiationN), ground heat flux (G), sensible heat flux (H), latent heat flux (LE), and evapotranspiration (ET). Each map includes a color scale that represents the range of measured values for the respective variable, and statistics such as median, mean, maximum, and minimum values are displayed above each map.

Scatter plot between the two dates for Rn, H, G, LE

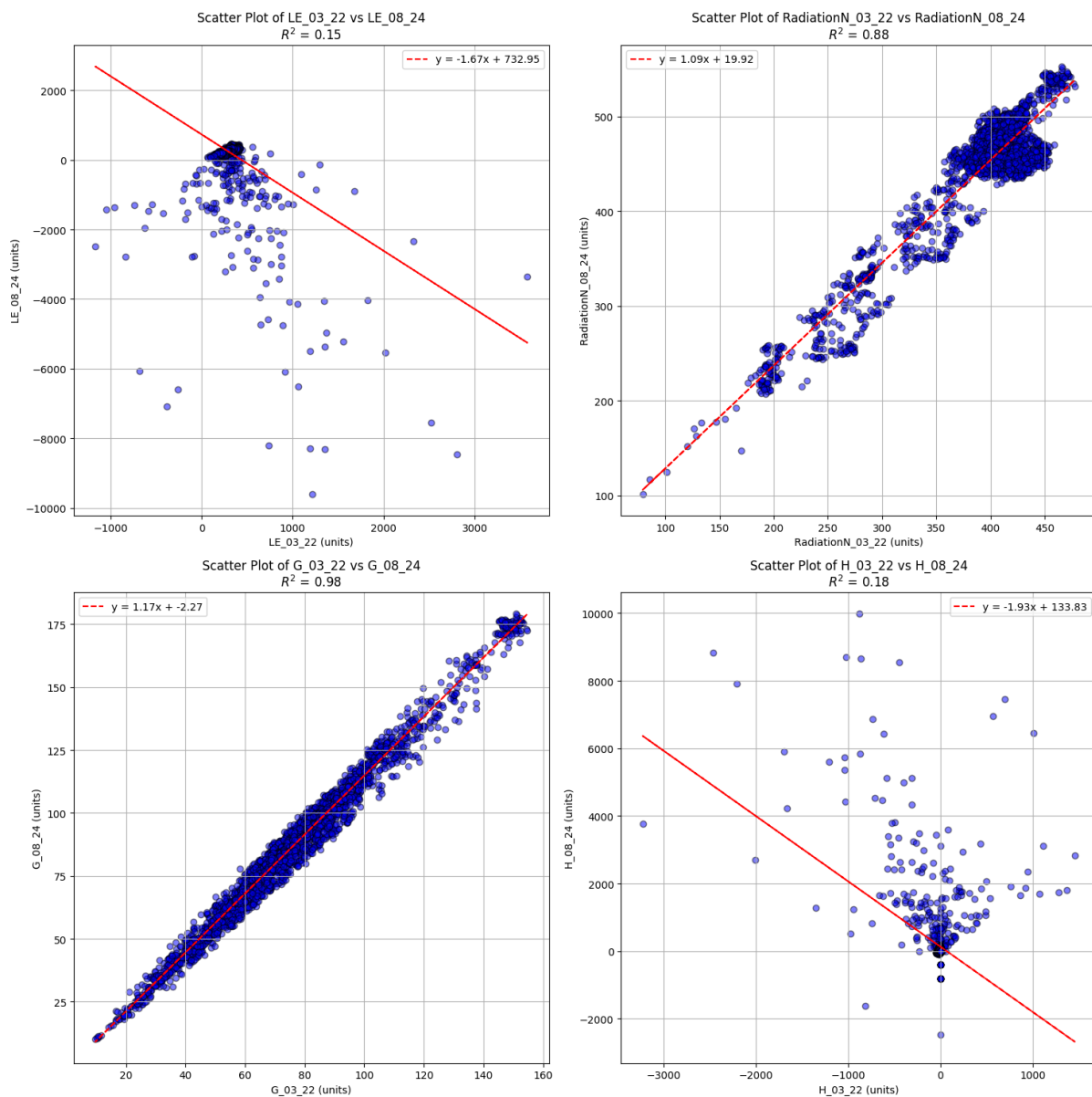


figure 3- scatter plot of Rn, G, H and LE

The figure shows four scatter plots comparing various energy variables between two dates: 03/22 and 08/24 2018. Each scatter plot illustrates the relationship between a variable on March 22 and the corresponding variable on August 24. each plot includes a linear regression line (in red), the equation of the line, and the R^2 value, which indicates the strength of the correlation between the two sets of data.

Scatter plot between the two dates for ET

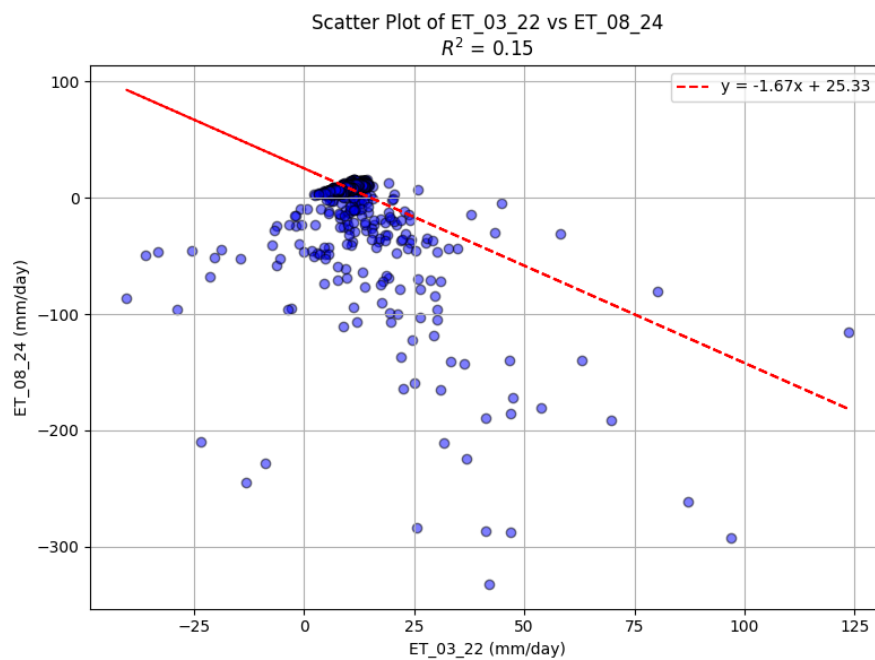


figure 4- scatter plot of ET

The scatter plot shows the relationship between evapotranspiration (ET) on March 22, 2018 (ET_03_22), and August 24, 2018 (ET_08_24). The x-axis represents ET values on March 22, while the y-axis represents ET values on August 24. A linear regression line is shown in red, with the equation $y = -1.67x + 25.33$ and an $R^2 = 0.15$ indicating a weak correlation between ET on the two dates.

4. Discussion

Maps:

Net Radiation (RadiationN): Net radiation is higher in August compared to March, likely due to seasonal differences. In summer, there are more daylight hours, and the sun is higher in the sky, leading to higher radiation values. The area around the Sea of Galilee shows different values compared to other regions, possibly due to the cooling and dispersing effects of the water, which influence radiation differently than the surrounding land.

Ground Heat Flux (G): The ground heat flux values are higher in August, particularly in open areas near the Mediterranean coastline. This corresponds to the expectation that the ground heats up more during the summer due to higher radiation. However, near water bodies, especially around the Sea of Galilee, there are areas where ground heat flux is lower, likely because the presence of water stabilizes temperatures in the nearby environment.

Sensible Heat Flux (H): In March, sensible heat flux values are lower, while in August there is a notable increase. This sharp rise reflects the significant heat stored in the ground during summer that is released into the atmosphere. Again, the influence of the Mediterranean Sea and the Sea of Galilee is apparent, with these areas showing lower flux values compared to the rest of the region.

Latent Heat Flux (LE): In March, latent heat flux is higher than in August, likely due to higher humidity and wetter soil conditions in the spring. In summer, as the ground dries out, latent heat flux decreases significantly. Proximity to water bodies affects these values, as areas near the Sea of Galilee and the coast maintain relatively high latent heat flux due to higher humidity in these areas.

Evapotranspiration (ET): Similar to latent heat flux, evapotranspiration values are higher in March, particularly in more humid areas. In summer, there is a sharp drop in ET values, especially in regions far from water bodies. In areas near the Mediterranean and the Sea of Galilee, evapotranspiration remains relatively high due to the moisture and proximity to water.

The Impact of Water Bodies: In all maps, two major water bodies can be identified—the Mediterranean Sea and the Sea of Galilee. The presence of these water bodies has clear spatial effects on the energy, heat, and evapotranspiration values. The water acts as a heat reservoir with a high thermal capacity, moderating temperature fluctuations and preventing sharp increases in ground and air temperatures. As a result, variables like sensible heat flux and net radiation are directly influenced by the proximity to water bodies, creating distinct patterns in these areas compared to regions farther from the water.

Nevertheless, there are some unusual findings:

Highly negative latent heat flux and evapotranspiration values in August, potentially indicating sensor issues or extremely dry conditions.

Very high sensible heat flux values in March, which are unusual for spring and could indicate localized extreme heating or data anomalies.

Unexpectedly high ground heat flux in certain areas in March, suggesting unusual heat retention in specific locations.

Coastal regions show greater shifts in ground heat flux between March and August, possibly influenced by unique land cover or soil properties.

These anomalies point to specific regions or conditions that may require further validation or study to ensure the accuracy of the data and to better understand the underlying environmental dynamics in these areas.

Scatter plots:

Evapotranspiration (ET): The scatter plot shows a weak negative correlation between ET on 03/22 and 08/24, with a $R^2 = 0.15$. The regression line indicates a downward trend, suggesting that areas with higher ET values in March tend to have lower ET values in August. This may be due to seasonal differences in moisture availability and vegetation cover.

Latent Heat Flux (LE) (Top left in second image): There is also a weak negative correlation $R^2 = 0.15$ between latent heat flux on 03/22 and 08/24, with a similar trend of decreasing values over time. This may reflect a reduction in available soil moisture or evapotranspiration capacity during the summer months.

Net Radiation (RadiationN) (Top right in the second image): This scatter plot shows a strong positive correlation ($R^2 = 0.88$) between net radiation on both dates. The slope of the regression line is close to 1, indicating that net radiation values are quite consistent between March and August, despite seasonal differences.

Ground Heat Flux (G) (Bottom left in second image): There is an extremely strong positive correlation ($R^2 = 0.98$) between ground heat flux on 03/22 and 08/24, with a near 1:1 ratio between the two dates. This suggests that the ground retains similar heat characteristics between seasons, although with some small increases in August.

Sensible Heat Flux (H) (Bottom right in second image): The sensible heat flux shows a weak negative correlation ($R^2=0.18$) between 03/22 and 08/24. This could indicate that while ground heat increases during summer, the transfer of heat into the atmosphere varies more significantly between seasons, likely influenced by atmospheric conditions and surface properties.

Overall Observations: The strongest correlations are observed in net radiation and ground heat flux, indicating that these variables remain relatively stable between March and August, likely due to consistent solar input and land surface characteristics. In contrast, evapotranspiration and latent heat flux show weaker correlations, likely due to seasonal changes in water availability and vegetation, while sensible heat flux demonstrates more variability in how heat is transferred into the atmosphere.

5. Conclusion

The data analysis reveals clear seasonal trends between March and August, affecting net radiation, ground heat flux, and sensible heat flux. During the summer, net radiation and ground heat flux are higher, particularly in open areas, due to longer daylight hours and a higher solar angle. Large water bodies, such as the Mediterranean Sea and the Sea of Galilee, influence these patterns by acting as heat reservoirs with high thermal capacity, which moderates temperature fluctuations and reduces heat fluxes in nearby regions.

In August, a notable increase in sensible heat flux was observed, while in March, higher values of latent heat flux and evapotranspiration (ET) were recorded, especially in more humid areas. Certain anomalies, such as negative latent heat flux values in August and unusually high values in March, may indicate measurement issues or unusual environmental conditions.

The scatter plot analysis indicates that net radiation and ground heat flux show the strongest correlations between seasons, suggesting relative stability of these variables. In contrast, evapotranspiration and latent heat flux exhibit greater variability between March and August, likely due to the impact of seasonal changes on water availability and vegetation.

In conclusion, the data highlights distinct seasonal processes in different regions, with significant influence from large water bodies on heat and moisture exchange dynamics. Further investigation is required to deepen understanding, utilizing remote sensing data and computational models to assess the impacts of climate change on water resources and vegetation. This can be especially valuable when integrated into decision support systems (DSS) for effective management of environmental challenges.

6. References

1. AghaKouchak, A, A Farahmand, F. S Melton, J Teixeira, M. C Anderson, B. D Wardlow, and C. R Hain. "Remote Sensing of Drought; Progress, Challenges, and Opportunities." *Reviews of Geophysics* 53, no. 2 (2015): 452–80.
2. Yuan, Qiangqiang, Huanfeng Shen, Tongwen Li, Zhiwei Li, Shuwen Li, Yun Jiang, Hongzhang Xu, et al. "Deep Learning in Environmental Remote Sensing: Achievements and Challenges." *Remote Sensing of Environment* 241 (2020): 111716-.
3. Dörnhöfer, Katja, and Natascha Oppelt. "Remote Sensing for Lake Research and Monitoring – Recent Advances." *Ecological Indicators* 64 (2016): 105–22.
<https://doi.org/10.1016/j.ecolind.2015.12.009>.